NRIAG JOURNAL OF ASTRONOMY AND GEOPHYSICS
2025, VOL. 14, NO. 1, 1–15
https://doi.org/10.1080/20909977.2025.2484132

Taylor & Francis
Taylor & Francis Group

OPEN ACCESS Check for updates

Two robust operational matrix algorithms for solving non-linear Lane–Emden-type equations in astrophysics using Hermite and Fermat polynomials

S. Krithikka and G Hariharan

Department of Mathematics, School of Arts, Sciences, Humanities and Education, SASTRA Deemed University, Thanjavur, India

ABSTRACT
Operational matrix-based algorithms have been identified as efficient tools for solving non-linear and fractional differential equations in engineering. Several wavelet-based algorithms have been developed for linear, non-linear and fractional differential equations. Wavelet-based spectral methods have also been identified as efficient tools for non-linear problems in astrophysics. In this paper, two reliable and efficient computational algorithms using Hermite wavelet and Fermat's polynomial collocation methods are introduced to solve a class of non-linear Lane–Emden-type equations in astrophysics. Lane–Emden models have been characterised to predict the dynamics in various astrophysical contexts, such as stellar structure, white dwarfs and polytropic models. The main idea of the proposed wavelet and spectral algorithms is that the non-linear singular differential equations are converted into a system of algebraic equations using the operational matrix of derivatives. To the best of our knowledge, so far no rigorous Hermite wavelet and Fermat's operational matrix of derivatives has been reported for the proposed models. The accuracy and efficiency of the proposed methods are confirmed by means of the comparison with other approximation algorithms. The proposed method can also be easily utilised to solve other types of non-linear differential equations in astrophysics.

ARTICLE HISTORY
Received 6 January 2025
Revised 4 March 2025
Accepted 20 March 2025

KEYWORDS
Astrophysics model; non-linear differential equations; Lane–Emden equation; Fermat's polynomials; Hermite wavelets; Hosoya polynomials

1. Introduction

Lane–Emden models are important phenomena in astrophysics, such as isotropic continuous media, isothermal gas spheres and the thermal behaviour of a spherical cloud of gas. Non-linear systems of Lane–Emden equations appear in the mathematical modelling of several physical problems, such as pattern formation, chemical reactions and population evolution. The study of fluid behaviour is crucial in astrophysics, influencing the formation of celestial bodies, galactic structures, accretion processes, explosive phenomena and interstellar material dynamics. Understanding the compressibility of astrophysical gases is essential, as they undergo significant density variations, unlike nearly incompressible liquids like water. Despite their particulate nature, gases are often treated as continuous media when particle distances are small compared to property variation scales, enabling consistent definitions of velocity and pressure while allowing for particle-level analysis when needed. Magnetic fields significantly impact many astrophysical environments, necessitating their inclusion in fluid dynamic models to ensure accurate representations of electromagnetic influences. Interestingly, astrophysical fluid dynamics share fundamental principles with ship dynamics, as both fields rely on fluid interactions – astrophysics focusing on gases and plasmas and ship dynamics dealing with water flow around vessels. Commonalities extend to wave dynamics, with gravitational waves studied in astrophysics paralleling water surface waves in naval engineering. Concepts such as hydrostatic equilibrium in stars and buoyancy in ships both involve force balances to maintain stability, while aerodynamics and drag reduction techniques are vital in both space and water environments. Moreover, magnetohydrodynamics (MHD) find applications in astrophysical plasma physics and ship propulsion technologies, with turbulence, vortex formation and energy transfer playing crucial roles in both disciplines.

Mathematical modelling provides a powerful tool for analysing astrophysical structures and stability, with the Lane–Emden equation serving as a fundamental non-linear differential equation describing polytropic stellar structures and self-gravitating systems. Originally introduced by Jonathan Homer Lane and Robert Emden, this equation has been extensively studied and adapted to address various astrophysical challenges. It effectively models density profiles in polytropic stars and gaseous celestial bodies, capturing essential non-linear behaviours under different conditions.

CONTACT G Hariharan hariharan@maths.sastra.edu Department of Mathematics, School of Arts, Sciences, Humanities and Education(SASHE), SASTRA Deemed University, Tirumalaisamudram,Thanjavur 613401, India

Researchers continue to refine numerical and analytical techniques for solving the Lane–Emden equation. Notably, Abu Arqub et al. (2013) introduced a residual power series (RPS) method for handling singular initial value problems, improving polynomial series solutions for stellar modelling. Parand et al. (2010) developed a Hermite collocation method that addresses equation singularities and accurately models astrophysical systems such as isothermal gas spheres. More recently, Gireesha and Gowtham (2024) proposed a hypergeometric wavelet method, enhancing computational efficiency and effectively managing singularities in density perturbation studies. Additional advanced approaches include the Fermat polynomial method by Nduka and Oruh (2022) for optimal astrophysical control solutions, while ZdeněkŠmarda (2015) proposed computational methods for solving singular initial value problems, offering deeper insights into stellar stability and density distributions. Baty (2023) demonstrated the potential of Physics-Informed Neural Networks (PINNs) in bridging data-driven and physics-based solutions to Lane–Emden-type equations. Analytical methods like the Differential Transform Method (DTM) have also been explored, with studies by Mukherjee and Roy (2011) and Biswas et al. (2023) showcasing its effectiveness in solving non-linear differential equations in astrophysical contexts. These diverse contributions highlight the Lane–Emden equation's adaptability across multiple astrophysical domains, including stellar evolution, oscillatory stability and modelling responses to external forces, reinforcing its role as a cornerstone in understanding the interplay of gravitational forces, density variations and thermal dynamics in self-gravitating systems. Ali (2019) has been used the Hybrid orthonormal Bernstein and block-pulse function wavelet method for Lane-emden type differential equations.

The Van der Pol (VdP) system has inspired many models in theoretical astrophysics, particularly in describing the dynamics of stellar oscillations and stability. A prominent example is the Lane–Emden equation, which models the density and pressure distribution within polytropic stars in hydrostatic equilibrium. This form of non-linear differential equation provides insight into the structural and oscillatory characteristics of self-gravitating fluids, analogous to how the VdP model provides a mathematical framework for studying ship roll dynamics.

The classical Lane–Emden equation for a spherically symmetric, self-gravitating, polytropic star is given by:

$$\frac{1}{\xi^2}\frac{d}{d\xi}\left(\xi^2\frac{d\theta}{d\xi}\right)+\theta^n=0,\ldots \tag{1.1}$$

where θ is a dimensionless density function that represents the ratio of the density at a given radius to the central density of the star. ξ is the dimensionless radial coordinate, which scales with the actual radius of the star. The polytropic index n describes the relationship between pressure and density in the polytropic gas.

To model analogous dynamics in the context of a ship's roll motion, we adopt modifications inspired by the Lane–Emden equation, introducing non-linear damping and restoring forces. To represent the asymmetric behaviour often observed in astrophysical systems, we adapt the Lane–Emden-based equation with terms that capture these asymmetries and the effects of external forces.

A modified form of the equation for non-linear oscillatory systems, comparable to ship roll dynamics, includes asymmetric damping terms and restoring forces. The equation is:

$$\frac{d^2(\phi)}{dt^2}+\beta(\phi^2-1)\left(\frac{d\phi}{dt}\right)+\left(\frac{\phi(\phi+\delta)(\phi+\varepsilon)}{\varepsilon\delta}\right)=\ldots \tag{1.2}$$

This modified equation is analogous to the Lane–Emden form, with β, the damping parameter, influencing the system's response to external forces, δ and ϵ, parameters introducing asymmetry in the restoring force, resembling the effects of fixed nodes and saddle points in the system.

To accommodate external disturbances – similar to gravitational perturbations or radioactive forces in astrophysical models – an external forcing term F(t) is added:

$$\frac{d^2(\phi)}{dt^2}+\beta(\phi-\nu_1)(\phi-\nu_2)\left(\frac{d\phi}{dt}\right)+\left(\frac{\phi(\phi+\delta)(\phi+\varepsilon)}{\varepsilon\delta}\right)=F(t) \tag{1.3}$$

with initial conditions:

$$\phi(0)=\phi_0,\left.\frac{d\phi}{dt}\right|_{t=0}=\phi_1 \tag{1.4}$$

Here, ϕ(t) signifies the angular displacement over time t, ν_1 and ν_2 introduce asymmetry in damping, which reflects varying energy dissipation, similar to the impact of polytropic indices on star stability, and F(t) represents an external excitation, analogous to forces acting on a self-gravitating system.

This research paper aims to further explore the application of the Lane–Emden non-linear equation in modelling ship roll dynamics. By investigating the effects of various parameters on the oscillator's behaviour, the study hopes to gain a deeper understanding of the factors that influence a ship's roll motion and their potential implications for ship stability.

In this study, two scenarios of ship roll dynamics without external forcing, which represent the natural, unexcited roll motion in steady-state, are considered. These scenarios are based on variations in the damping coefficient β, which modifies the roll damping, and different values of constants ν_1 and ν_2, representing an asymmetric damping term related to the non-linear dissipation in the Lane–Emden equations. Fixed values of ϵ, which is used to control the period of roll oscillations, and δ, a coefficient of the cubic restoring term that replaces the harmonic restoring force of the classical form of the equation, are also considered.

This study aims to explore how these parameters affect the roll dynamics, with particular attention to stability and potential instabilities, such as parametric roll, which can occur under certain sea conditions. Understanding these dynamics is critical for improving ship design and enhancing safety during maritime operations.

Wavelets provide a powerful tool for multi-resolution analysis by scaling and translating functions, making them especially effective in representing functions with sharp changes or localised features. Unlike traditional Fourier methods, which are well suited for periodic and smooth functions, wavelets are particularly advantageous for handling the complexities of non-linear ordinary (ODEs), partial (PDEs) and fractional differential equations (FDEs). The application of wavelet methods in solving such equations represents a major advancement in numerical analysis, offering a flexible and efficient approach to dealing with complex dynamical systems found in fields like physics, engineering, biology and finance, where traditional methods often struggle with inherent nonlinearities.

Among wavelet methods, the Fermat wavelet method stands out due to its use of Fermat polynomials, which possess strong recurrence relations and are well suited for solving non-linear differential equations. These wavelets inherit beneficial properties such as stability and adaptability, making them effective for numerical analysis. The Fermat wavelet method involves employing operational matrices of derivatives to transform non-linear differential equations into a system of algebraic equations, solvable using standard numerical techniques.

Numerous studies have highlighted the application of wavelet-based methods to address complex computational problems. For example, the Hermite wavelet method (HWM), utilising Hermite polynomials known for their orthogonality and ability to represent localised features, has been applied to non-linear and fractional differential equations. The Hosoya polynomial method (HPM) is another significant contribution, leveraging the recurrence relations of Hosoya polynomials to efficiently solve non-linear ordinary and partial differential equations. These methods provide alternative approaches to solving Lane–Emden equations and similar non-linear models.

Fermat and Hermite wavelet algorithms with suitable collocation points have been used to get lower computation costs. For the first time, these algorithms have been applied to get more accurate results than the other algorithms (as per the specific applications). We have validated the results with FPM, HWM and HPM.

This paper is organised as follows: in Section 2, orthogonal polynomials and wavelets are presented. Numerical experiments are discussed in Section 3. Results and discussion are given in Section 4. Concluding remarks are provided in Section 5.

2. Orthogonal polynomials and wavelets

2.1. Fermat Polynomials

Fermat polynomials can be generated by the recurrence relation:

$$F_{i+2}(x) = 3xF_{i+1}(x) - 2F_i(x); F_0(x) = 0, F_1(x) = 1, i \geq 0 \tag{2.1.1}$$

These polynomials are specific instances of the (p,q)-Fibonacci polynomials, introduced in reference Youssri (2017). The general form of these polynomials is generated by the relation:

$$U_{i+2}(x) = p(x)U_{i+1}(x) - q(x)U_i(x), i \geq 0$$

with initial conditions:

$$U_0(x) = 0, U_1(x) = 1$$

The Binet formula for $U_i(x)$ is given by

$$U_i(x) = \frac{\propto^i(x) - \beta^i(x)}{\alpha(x) - \beta(x)},$$

where:

$$\alpha(x) = \frac{p(x) + \sqrt{p(x)^2 + 4q(x)}}{2},$$
$$\beta(x) = \frac{p(x) - \sqrt{p(x)^2 + 4q(x)}}{2}$$

For Fermat polynomials, we use p(x) = 3× and q(x) = −2.

In this work, Fermat polynomials are defined on the domain x∈[0,1] with their explicit form given by

$$F_k(x) = \frac{\left(3x+\sqrt{9x^2-8}\right)^k - \left(3x-\sqrt{9x^2-8}\right)^k}{2^k\sqrt{9x^2-8}}$$

The polynomials $F_{i+1}(x)$ have the following analytic form:

$$F_{i+1}(x) = \sum_{k=0}^{i/2}(-2)^k 3^{i-2k}\binom{i-k}{k}x^{i-2k}.$$

Operational matrices of derivative D and D^2 by Fermat polynomial method are

$$D = \begin{bmatrix} 0 & 0 & 0 \\ 3 & 0 & 0 \\ 0 & 6 & 0 \end{bmatrix}, D^2 = \begin{bmatrix} 0 & 0 & 0 \\ 0 & 0 & 0 \\ 0 & 36 & 0 \end{bmatrix}$$

Then the Fermat polynomial matrix is

$$\psi(x) = \begin{bmatrix} 1 \\ 3x \\ 9x^2-2 \end{bmatrix}$$

2.1.1. Convergence analysis

The convergence of the parameterisation method typically relies on the Weierstrass Approximation Theorem, which has been extensively validated by numerous scholars.

Theorem 2.1: Weierstrass Approximation Theorem

Let $f\varepsilon C([a,b],\mathbb{R})$. Then, there is a sequence of polynomials, $P_n(x)$ that converges to f(x) on [a, b].

Proof: Refer [5]

Theorem 2.2: *If* $\alpha_n = inf_{Q_n}J$, *for* n = 1,2, ..., *then* $\lim_{n\to\infty}\alpha_n$ *where* $\alpha = inf_Q J$.

Proof: Refer [5]

2.2. Wavelets and Hermite wavelets

In recent years, wavelets have found their way into many different fields of science and engineering. Wavelets constitute a family of functions constructed from the dilation and translation of a single function called the mother wavelet. When the dilation parameter a and the translation parameter b vary continuously, we have the following family of continuous wavelets,

$$\psi_{a,b}(t) = |a|^{\frac{-1}{2}}\psi\left(\frac{t-b}{a}\right) \quad a,b\in R, a\neq 0.$$

2.2.1. Functions approximation

A function f(t) defined over [0,1) may be expanded as

$$f(t) = \sum_{n=1}^{\infty}\sum_{m=0}^{\infty}c_{nm}\psi_{nm}(t)$$

where $c_{nm} = \langle f(t), \psi_{nm}(t)\rangle$, in which $\langle .,.\rangle$ denotes the inner product. If the infinite series in is truncated, then it can be written as

$$f(t) = \sum_{n=1}^{2^{k-1}}\sum_{m=0}^{M-1}c_{nm}\psi_{nm}(t)$$

It can be written as

$$f(t) = \sum_{n=1}^{2^{k-1}}\sum_{m=0}^{M-1}c_{nm}\psi_{nm}(t) = C^T\psi(t)$$

where C *and* $\psi(t)$ *are* $2^{k-1}M\times 1$ matrices given as

$$C = \begin{bmatrix} c_{10}, c_{11}, \ldots, c_{1M-1}, c_{20}, c_{21}, \ldots . \\ c_{2M-1}, \ldots, c_{2^{k-1}0}, \ldots, c_{2^{k-1}M-1} \end{bmatrix}^T$$

and

$$\psi(t) = \begin{bmatrix} \psi_{10}, \psi_{11}, \ldots, \psi_{1M-1}, \psi_{20}, \psi_{21}, \ldots, \\ \psi_{2M-1}, \ldots, \psi_{2^{k-1}0}, \ldots, \psi_{2^{k-1}M-1} \end{bmatrix}^T$$

2.2.2. Convergence analysis

Let $L^2([0,1])$ be a Hilbert space for which $\psi_{n,m}(x)$ form an orthonormal sequence in $L^2([0,1])$

Let $y(x)\in L^2([0,1])$ we have

$$y(x) = \sum_{n=1}^{2^{k-1}}\sum_{m=0}^{M-1}a_{nm}\psi_{n,m}(x)$$

where $anm = \left\langle y(x), \psi_{n,m}(x)\right\rangle$ is an inner product of $y(x)$ and $\psi_{n,m}(x)$

It can be written as

$$y(x)\sum_{n=1}^{2^{k-1}}\sum_{m=0}^{M-1} < y(x), \psi_{n,m}(x) > \psi_{n,m}(x)$$

For simplicity, Let j = M(n-1)+m + 1;

$$y(x) = \sum_{j=1}^{\hat{m}}\left\langle y(x),\ \psi_j(x)\right\rangle\psi_j(x)$$
$$= \sum_{j=1}^{\hat{m}}a_j\psi_j(x) = a^T\psi(x)$$

Since $= 2^{k-1}M$ and method converges if $\to\infty$; that is when we use higher-order Hermite polynomials M-1 or use higher level of resolution k or use both higher M and k, we get more accurate results.

where $a_j = a_{mn},\ \psi_j(x) = \psi_{m,n}(x), = 2^{k-1}M$ and $a = [a_1, a_2, \ldots\ldots\ldots a]^T$

By taking the procedure, we obtained the convergence of all orthogonal wavelet methods for all levels of resolution k, that is, $\sum_{j=1} a_j\psi_j(x)$ converges to y(x), as $\to\infty$

Let the derivative of the wavelet vector be expressed as

$$\frac{d\psi(x)}{dx} \approx D\psi(x),$$

where D is the operational matrix of the derivative.

To compute D, the relationship between Hermite wavelets and their derivatives is used. The derivative of the Hermite polynomials follows:

$$\dot{H}_{m+1}(x) = 2(m+1)H_m(x),$$

$$\dot{\psi}_{n,m+1}(x) = 2^k(m+1)\psi_{n,m}(x).$$

The matrix D is then expressed as a block diagonal matrix:

$$D = \left(\begin{bmatrix} w & 0 & \cdots & 0 \\ 0 & w & \cdots & 0 \\ \vdots & \vdots & \ddots & \vdots \\ 0 & 0 & \cdots & w \end{bmatrix}\right),$$

where W is a square matrix given by:

$$W = 2^k \left(\begin{bmatrix} 0 & 0 & 0 & \cdots & 0 \\ 1 & 0 & 0 & \cdots & 0 \\ 0 & 2 & 0 & \cdots & 0 \\ \vdots & \vdots & \vdots & \ddots & 0 \\ 0 & 0 & 0 & \cdots & (M-1) \end{bmatrix}\right).$$

Here k is the level of Hermite wavelet, and M is the number of Hermite polynomials considered.

Operational matrices of derivative D and D^2 by Hermite wavelet method are

$$D = \begin{bmatrix} 0 & 0 & 0 \\ 4 & 0 & 0 \\ 0 & 8 & 0 \end{bmatrix}, D^2 = \begin{bmatrix} 0 & 0 & 0 \\ 0 & 0 & 0 \\ 32 & 0 & 0 \end{bmatrix}$$

Then the Hermite wavelet matrix is

$$\psi(x) = \frac{2}{\sqrt{\pi}} \begin{bmatrix} 1 \\ 4x-1 \\ 16x^2-16x+2 \end{bmatrix}$$

3. Numerical solutions

Problem 1:

$$y^{II}(x) + \frac{8}{x} y^I(x) + xy(x) = x^5 - x^4 + 44x^2 - 30x, \\ ; x \geq 0 \tag{3.49}$$

with the initial boundary value condition

$y(0) = 0 and y^I(0) = 0$.

The exact solution for the above Lane–Emden equation is $y(x) = x^4 - x^3$.

Equations of this form have been solved using the Fermat polynomial method (FPM), Hermite

wavelet method (HWM) and Hosoya polynomial method (HPM) with error computation

included to assess solution accuracy.

3.1. FPM

The FPM is stated as

$$\begin{aligned} &108C_2x + \frac{8}{x}(3C_1 + 18C_2x) \\ &+ x\left[C_0 + 3C_1x + \left(9x^2-2\right)C_2\right] \\ &= x^5 - x^4 + 44x^2 - 30x \end{aligned} \tag{3.2}$$

Considering collocation point as × = 0.47, utilising the Fermat polynomial operational matrices of derivatives, we derive the subsequent algebraic equation

$$0.47C_0 + 51.72C_1 + 194.745C_2 = -4.40 \tag{3.3}$$

Under the given boundary value conditions we have the following equations,

$$y(0) = 0 \Rightarrow C_0 - 2C_2 = 0 \Rightarrow C_0 = 2C_2; \tag{3.4}$$

$$y^I(0) = 0C_1 = 0 \tag{3.5}$$

Therefore by solving Equations (3.3), (3.4) and (3.5), we get $C_0 = -0.04, C_1 = 0, C_2 = -0.02$

Hence we get the Fermat polynomial solution by utilising the above connection coefficients as

$$\boldsymbol{y(x) = 0 - 0.18x^2} \tag{3.6}$$

3.2. HWM

The HWM is stated as

$$\begin{aligned} &32C_2 + \frac{8}{x}(4C_1 + C_2(32x-16)) \\ &+ x\left[C_0 + C_1(4x-2) + \left(16x^2 - 16x + 2\right)C_2\right] \\ &= x^5 - x^4 + 44x^2 - 30x \end{aligned} \tag{3.7}$$

Considering collocation point as x = 0.5, utilising the Hermite wavelet operational matrices of derivatives, we derive the subsequent algebraic equation

$$0.5C_0 + 64C_1 + 31C_2 = -4.03 \tag{3.8}$$

Under the given boundary value conditions, we have the following equations,

$$y(0) = 0 \Rightarrow C_0 - 6C_2 = 0 \Rightarrow C_0 = 6C_2; \tag{3.9}$$

$$y^I(0) = 0C_1 - 4C_2 = 0C_1 = 4C_2 \tag{3.10}$$

Therefore by solving Equations (3.8), (3.9) and (3.10), we get

$$C_0 = -0.06, C_1 = -0.04, C_2 = -0.01$$

Hence we get the Hermite wavelet solution by utilising the above connection coefficients as

$$\boldsymbol{y(x) = 0 - 0.16x^2} \tag{3.11}$$

3.3. HPM

The HPM is stated as

$$2C_2+\frac{8}{x}(C_1+2C_2(x-1)) \\ +x\left[C_0+C_1(x+2)+\left(x^2+2x+3\right)C_2\right] \\ =x^5-x^4+44x^2-30x \quad (3.12)$$

Considering collocation point as$x=-2$, utilising the Hosoya polynomial operational matrices of derivatives, we derive the subsequent algebraic equation

$$-2C_0-4C_1+20C_2=188 \quad (3.13)$$

Under the given boundary value conditions, we have the following equations,

$$y(0)=0\Rightarrow C_0+7C_2=0\Rightarrow C_0=-7C_2; \quad (3.14)$$

$$y^I(0)=0C_1-2C_2=0C_1=2C_2 \quad (3.15)$$

Therefore by solving Equations (3.13), (3.14) and (3.15), we get

$$C_0=-50.61, C_1=14.46, C_2=7.23$$

Hence we get the Hosoya polynomial solution by utilising the above connection coefficients as

$$\boldsymbol{y(x)=0+28.92x+7.23x^2} \quad (3.16)$$

Problem 2:

$$y^{II}(x)+\frac{2}{x}y^I(x)+y(x)=6+2x+x^2+x^3,;x\geq 0 \quad (3.17)$$

with the initial boundary value conditions $y(0)=0 and y^I(0)=0$. The exact solution for the above Lane–Emden equation is $y(x)=x^2+x^3$. Equations of this form have been solved using the Fermat polynomial method (FPM), Hermite

wavelet method (HWM) and Hosoya polynomial method (HPM) with error computation

included to assess solution accuracy.

3.4. FPM

The FPM is stated as

$$108C_2x+\frac{2}{x}(3C_1+18C_2x) \\ +\left[C_0+3C_1x+\left(9x^2-2\right)C_2\right] \\ =6+2x+x^2+x^3 \quad (3.18)$$

Considering collocation point as x = 0.47, utilising the Fermat polynomial operational matrices of derivatives, we derive the subsequent algebraic equation

$$C_0+14.176C_1+86.7481C_2=11.96 \quad (3.19)$$

Under the given boundary value conditions, we have the following equations,

$$y(0)=0\Rightarrow C_0-2C_2=0\Rightarrow C_0=2C_2; \quad (3.20)$$

$$y^I(0)=0C_1=0 \quad (3.21)$$

Therefore by solving Equations (3.19), (3.20) and (3.21), we get $C_0=0.26, C_1=0, C_2=0.13$
Hence we get the Fermat polynomial solution by utilising the above connection coefficients as

$$\boldsymbol{y(x)}=0+1.17\boldsymbol{x}^2 \quad (3.22)$$

3.5. HWM

The HWM is stated as

$$32C_2+\frac{2}{x}(4C_1+C_2(32x-16)) \\ +\left[C_0+C_1(4x-2)+\left(16x^2-16x+2\right)C_2\right] \\ =6+12x+x^2+x^3 \quad (3.23)$$

Considering collocation point as x = 0.5, utilising the Hermite wavelet operational matrices of derivatives, we derive the subsequent algebraic equation

$$C_0+16C_1+30C_2=12.375 \quad (3.24)$$

Under the given boundary value conditions, we have the following equations,

$$y(0)=0\Rightarrow C_0-6C_2=0\Rightarrow C_0=6C_2; \quad (3.25)$$

$$y^I(0)=0C_1-4C_2=0C_1=4C_2 \quad (3.26)$$

Therefore by solving Equations (3.24), (3.25) and (3.26), we get

$$C_0=0.72, C_1=0.48, C_2=0.12$$

Hence we get the Hermite wavelet solution by utilising the above connection coefficients as

$$\boldsymbol{y(x)}=0+1.9\boldsymbol{x}^2 \quad (3.27)$$

3.6. HPM

The HPM is stated as

$$2C_2+\frac{2}{x}(C_1+2C_2(x-1)) \\ +\left[C_0+C_1(x+2)+\left(x^2+2x+3\right)C_2\right] \\ =6+12x+x^2+x^3 \quad (3.28)$$

Considering collocation point as$x=-2$, utilising the Hosoya polynomial operational matrices of derivatives, we derive the subsequent algebraic equation

$$-3C_0-C_1+9C_2=-22 \quad (3.29)$$

Under the given boundary value conditions, we have the following equations,

$$y(0)=0\Rightarrow C_0+7C_2=0\Rightarrow C_0=-7C_2; \quad (3.30)$$

$$y^I(0)=0\Rightarrow C_1-2C_2=0\Rightarrow C_1=2C_2 \quad (3.31)$$

Therefore by solving Equations (3.29), (3.30) and (3.31), we get $C_0 = -10.99, C_1 = 3.14, C_2 = 1.57$
Hence we get the Hosoya polynomial solution by utilising the above connection coefficients as

$$\boldsymbol{y}(\boldsymbol{x}) = 0 + 6.28\boldsymbol{x} + 1.57\boldsymbol{x}^2 \quad (3.32)$$

Problem 3:

$$y^{II}(x) + \frac{6}{x}y^{I}(x) + 14y(x) + 4y(x)\log(y(x)) = 0, ; x \geq 0 \quad (3.33)$$

with the initial boundary value condition $y(0) = 1 and y^{I}(0) = 0$. The exact solution for the above Lane–Emden equation is $y(x) = e^{-x^2}$.
Equations of this form have been solved using the Fermat polynomial method (FPM), Hermite wavelet method (HWM) and Hosoya polynomial method (HPM) with error computation included to assess solution accuracy.

3.7. FPM

The FPM is stated as

$$108C_2x + \frac{6}{x}(3C_1 + 18C_2x) + 14\left[C_0 + 3C_1x + \left(9x^2 - 2\right)C_2\right] + 4\left[C_0 + 3C_1x + \left(9x^2 - 2\right)C_2\right] \log\left\{\left[C_0 + 3C_1x + \left(9x^2 - 2\right)C_2\right]\right\} = 0 \quad (3.34)$$

Considering collocation point as x = 0.47, utilising the Fermat polynomial operational matrices of derivatives, we derive the subsequent algebraic equation

$$18C_0 + 63.67C_1 + 158.59C_2 - 0.04\log(C_0 + 1.41C_1 - 0.0119C_2) = 0 \quad (3.35)$$

Under the given boundary value conditions, we have the following equations

$$y(0) = 1 \Rightarrow C_0 - 2C_2 = 1 \Rightarrow C_0 = 1 + 2C_2; \quad (3.36)$$

$$y^{I}(0) = 0C_1 = 0 \quad (3.37)$$

Therefore by solving Equations (3.35), (3.36) and (3.37), we get

$$C_0 = 0.82, C_1 = 0, C_2 = -0.09$$

Hence we get the Fermat polynomial solution by utilising the above connection coefficients as

$$\boldsymbol{y}(\boldsymbol{x}) = 1 - 0.81\boldsymbol{x}^2 \quad (3.38)$$

3.8. HWM

The HWM is stated as

$$32C_2 + \frac{6}{x}(4C_1 + C_2(32x - 16)) + 14\left[C_0 + C_1(4x - 2) + \left(16x^2 - 16x + 2\right)C_2\right] + 4\left[C_0 + C_1(4x - 2) + \left(16x^2 - 16x + 2\right)C_2\right] \log\left\{\left[C_0 + C_1(4x - 2) + \left(16x^2 - 16x + 2\right)C_2\right]\right\} = 0 \quad (3.39)$$

Considering collocation point as x = 0.5, utilising the Hermite wavelet operational matrices of derivatives, we derive the subsequent algebraic equation

$$18C_0 + 48C_1 + 4C_2 - 8C_2log(C_0 - 2C_2) = 0 \quad (3.40)$$

Under the given boundary value conditions, we have the following equations,

$$y(0) = 1 \Rightarrow C_0 - 6C_2 = 1 \Rightarrow C_0 = 1 + 6C_2; \quad (3.41)$$

$$y^{I}(0) = 0C_1 - 4C_2 = 0C_1 = 4C_2 \quad (3.42)$$

Therefore by solving Equations (3.40), (3.41) and (3.42), we get

$$C_0 = 0.7, C_1 = -0.2, C_2 = -0.05$$

Hence, we get the Hermite wavelet solution by utilising the above connection coefficients as

$$\boldsymbol{y}(\boldsymbol{x}) = 1 - 0.8\boldsymbol{x}^2 \quad (3.43)$$

3.9. HPM

The HPM is stated as

$$2C_2 + \frac{6}{x}(C_1 + 2C_2(x - 1)) + 14\left[C_0 + C_1(x + 2) + \left(x^2 + 2x + 3\right)C_2\right] + 4\left[C_0 + C_1(x + 2) + \left(x^2 + 2x + 3\right)C_2\right] log\left\{\left[C_0 + C_1(x + 2) + \left(x^2 + 2x + 3\right)C_2\right]\right\} = 0 \quad (3.44)$$

Considering collocation point asx = −2, utilising the Hosoya polynomial operational matrices of derivatives, we derive the subsequent algebraic equation

$$14C_0 - 3C_1 + 8C_2 + 4(C_0 + 3C_2)log(C_0 + 3C_2) = 0 \quad (3.45)$$

Under the given boundary value conditions, we have the following equations,

$$y(0) = 1 \Rightarrow C_0 + 7C_2 = 1 \Rightarrow C_0 = 1 - 7C_2; \quad (3.46)$$

$$y^{I}(0) = 0C_1 - 2C_2 = 0C_1 = 2C_2 \quad (3.47)$$

Therefore by solving Equations (3.28) and (3.29), we get $C_0 = -0.68, C_1 = 0.48, C_2 = 0.24$

Hence we get the Hosoya polynomial solution by utilising the above connection coefficients as

$$\boldsymbol{y}(\boldsymbol{x}) = 1 + 0.96\boldsymbol{x} + 0.24\boldsymbol{x}^2 \tag{3.48}$$

Problem 4:

$$y^{II}(x) + \frac{10}{x}y^{I}(x) + y^{10}(x) = x^{100} + 190x^8; 0 \le x \le 1 \tag{3.49}$$

with the initial boundary value condition $y(0) = 0, y^I(0) = 0$. The exact solution for the above Lane–Emden equation is $y(x) = x^{10}$.
Equations of this form have been solved using the Fermat polynomial method (FPM), Hermite wavelet method (HWM) and Hosoya polynomial method (HPM) with error computation included to assess solution accuracy.

3.10. FPM

The FPM is stated as

$$108C_2x + \frac{10}{x}(3C_1 + 18C_2x) + \left[C_0 + 3C_1x + \left(9x^2 - 2\right)C_2\right]^{10} = x^{100} + 190x^8 \tag{3.50}$$

Considering collocation point as x = 0.47, utilising the Fermat polynomial operational matrices of derivatives, we derive the subsequent algebraic equation

$$(C_0 + 1.41C_1 - 0.0119C_2)^{10} + 63.82C_1 + 230.76C_2 = 0.45 \tag{3.51}$$

Under the given boundary value condition, we have the following equations,

$$y(0) = 0 \Rightarrow C_0 - 2C_2 = 0 \Rightarrow C_0 = 2C_2 \tag{3.52}$$

$$y^I(0) = 0C_1 = 0 \tag{3.53}$$

Therefore by solving the system of algebraic equations, we get

$$C_0 = 0.004, C_1 = 0, C_2 = 0.002$$

Hence we get the Fermat polynomial solution by utilising the above connection coefficients as

$$\boldsymbol{y}(\boldsymbol{x}) = 0 + 0.018\boldsymbol{x}^2 \tag{3.54}$$

3.11. HWM

The HWM is stated as

$$32C_2 + \frac{10}{x}(4C_1 + C_2(32x - 16)) + \left[C_0 + C_1(4x - 2) + \left(16x^2 - 16x + 2\right)C_2\right]^{10} = x^{100} + 190x^8 \tag{3.55}$$

Considering collocation point as x = 0.5, utilising the Hermite wavelet operational matrices of derivatives, we derive the subsequent algebraic equation

$$(C_0 - 2C_2)^{10} + 80C_1 + 32C_2 = 0.74 \tag{3.56}$$

Under the given boundary value conditions, we have the following equations,

$$y(0) = 0 \Rightarrow C_0 - 6C_2 = 0 \Rightarrow C_0 = 6C_2; \tag{3.57}$$

$$y^I(0) = 0C_1 - 4C_2 = 0C_1 = 4C_2 \tag{3.58}$$

Therefore by solving the system of algebraic equations, we get

$$C_0 = 0.012, C_1 = 0.008, C_2 = 0.002$$

Hence we get the Hermite wavelet solution by utilising the above connection coefficients as

$$\boldsymbol{y}(\boldsymbol{x}) = 0 + 0.032\boldsymbol{x}^2 \tag{3.59}$$

3.12. HPM

The HPM is stated as

$$2C_2 + \frac{10}{x}(C_1 + 2C_2(x - 1)) + \left[C_0 + C_1(x + 2) + \left(x^2 + 2x + 3\right)C_2\right]^{10} = x^{100} + 190x^8 \tag{3.60}$$

Considering collocation point as x = −2, utilising the Hosoya polynomial operational matrices of derivatives, we derive the subsequent algebraic equation

$$(C_0 + 3C_2)^{10} - 5C_1 + 32C_2 = 126750 \tag{3.61}$$

Under the given boundary value conditions, we have the following equations,

$$y(0) = 0 \Rightarrow C_0 + 7C_2 = 0 \Rightarrow C_0 = -7C_2; \tag{3.62}$$

$$y^I(0) = 0C_1 - 2C_2 = 0C_1 = 2C_2 \tag{3.63}$$

Therefore by solving the system of algebraic equations, we get

$$C_0 = -1792, C_1 = 512, C_2 = 256$$

Hence we get the Hosoya polynomial solution by utilising the above connection coefficients as

$$\boldsymbol{y}(\boldsymbol{x}) = 0 + 1024\boldsymbol{x} + 256\boldsymbol{x}^2 \tag{3.64}$$

Problem5:

$$y^{II}(x)+\frac{2}{x}y^{I}(x)+y(x)=0; x\geq 0 \quad (3.65)$$

with the initial boundary value condition $y(0)=1, y^{I}(0)=0$. The exact solution for the above Lane–Emden equation is $y(x)=\frac{sinx}{x}$.
Equations of this form have been solved using the Fermat polynomial method (FPM), Hermite wavelet method (HWM) and Hosoya polynomial method (HPM) with error computation included to assess solution accuracy.

3.13. FPM

The FPM is stated as

$$108C_2x+\frac{2}{x}(3C_1+18C_2x)+\left[C_0+3C_1x+\left(9x^2-2\right)C_2\right]=0 \quad (3.66)$$

Considering collocation point as x = 0.47, utilising the Fermat polynomial operational matrices of derivatives, we derive the subsequent algebraic equation

$$C_0+14.17C_1+86.76C_2=0 \quad (3.67)$$

Under the given boundary value conditions, we have the following equations,

$$y(0)=1\Rightarrow C_0-2C_2=1\Rightarrow C_0=1+2C_2; \quad (3.68)$$

$$y^{I}(0)=0C_1=0 \quad (3.69)$$

Therefore by solving the system of algebraic equations, we get

$$C_0=0.98, C_1=0, C_2=-0.01$$

Hence we get the Fermat polynomial solution by utilising the above connection coefficients as

$$\boldsymbol{y}(\boldsymbol{x})=1-0.18\boldsymbol{x}^2 \quad (3.70)$$

3.14. HWM

The HWM is stated as

$$32C_2+\frac{2}{x}(4C_1+C_2(32x-16))+\left[C_0+C_1(4x-2)+\left(16x^2-16x+2\right)C_2\right]=0 \quad (3.71)$$

Considering collocation point as x = 0.5, utilising the Hermite wavelet operational matrices of derivatives, we derive the subsequent algebraic equation

$$C_0+16C_1+3C_2= \quad (3.72)$$

Under the given boundary value conditions, we have the following equations,

$$y(0)=1\Rightarrow C_0-6C_2=1\Rightarrow C_0=1+6C_2; \quad (3.73)$$

$$y^{I}(0)=0C_1-4C_2=0C_1=4C_2 \quad (3.74)$$

Therefore by solving the system of algebraic equations, we get

$$C_0=0.94, C_1=-0.04, C_2=-0.01$$

Hence we get the Hermite wavelet solution by utilising the above connection coefficients as

$$\boldsymbol{y}(\boldsymbol{x})=1-0.16\boldsymbol{x}^2 \quad (3.75)$$

3.15. HPM

The HPM is stated as

$$2C_2+\frac{2}{x}(C_1+2C_2(x-1))+\left[C_0+C_1(x+2)+\left(x^2+2x+3\right)C_2\right]=0 \quad (3.76)$$

Considering collocation point as x = −2, utilising the Hosoya polynomial operational matrices of derivatives, we derive the subsequent algebraic equation

$$C_0-C_1+11C_2=0 \quad (3.77)$$

Under the given boundary value conditions, we have the following equations,

$$y(0)=1\Rightarrow C_0+7C_2=1\Rightarrow C_0=1-7C_2; \quad (3.78)$$

$$y^{I}(0)=0C_1-2C_2=0C_1=2C_2 \quad (3.79)$$

Therefore by solving the system of algebraic equations, we get

$$C_0=4.5, C_1=-1, C_2=-0.5$$

Hence we get the Hosoya polynomial solution by utilising the above connection coefficients as

$$\boldsymbol{y}(\boldsymbol{x})=1-2\boldsymbol{x}-0.5\boldsymbol{x}^2 \quad (3.80)$$

4. Results and discussion

Tables 1–5 show the comparative study of the proposed wavelet based methods and polynomial approximation methods such as HPM and FPM. For small values of k and M, the proposed results are validated with other results. Figures 1–5 show the accuracy of the proposed method. The accuracy has been confirmed by means of computing errors. The graphical representation (Figure 6) of the error metrics gives us a clear view that the errors of FPM and HWM are minimum compared to the HPM. Tables 6–8 provide the complete information

Table 1. Comparing absolute error of an approximate solution with the exact solution for problem 1.

x	Exact value	FPM	HWM	HPM	Error (FPM)	Error (HWM)	Error (HPM)
0.00	0	0	0	0	0	0	0
0.01	−9.9E−07	−8.1E−05	−1.6E−05	0.289923	0.00008001	0.00001501	0.28992399
0.02	−7.84E−06	−0.00032	−6.4E−05	0.581292	0.00031616	0.00005616	0.58129984
0.03	−2.619E−05	−0.00073	−0.00014	0.874107	0.00070281	0.00011781	0.87413319
0.04	−6.144E−05	−0.0013	−0.00026	1.168368	0.00123456	0.00019456	1.16842944
0.05	−0.0001188	−0.00203	−0.0004	1.464075	0.00190625	0.00028125	1.46419375
0.06	−0.000203	−0.00292	−0.00058	1.761228	0.00271296	0.00037296	1.76143104
0.07	−0.000319	−0.00397	−0.00078	2.059827	0.00365001	0.00046501	2.06014599
0.08	−0.000471	−0.00518	−0.00102	2.359872	0.00471296	0.00055296	2.36034304
0.09	−0.0006634	−0.00656	−0.0013	2.661363	0.00589761	0.00063261	2.66202639
0.10	−0.0009	−0.0081	−0.0016	2.9643	0.0072	0.0007	2.9652
0.20	−0.0064	−0.0324	−0.0064	6.0732	0.026	8.6736E−19	6.0796
0.30	−0.0189	−0.0729	−0.0144	9.3267	0.054	0.0045	9.3456
0.40	−0.0384	−0.1296	−0.0256	12.7248	0.0912	0.0128	12.7632
0.50	−0.0625	−0.2025	−0.04	16.2675	0.14	0.0225	16.33
0.60	−0.0864	−0.2916	−0.0576	19.9548	0.2052	0.0288	20.0412
0.70	−0.1029	−0.3969	−0.0784	23.7867	0.294	0.0245	23.8896
0.80	−0.1024	−0.5184	−0.1024	27.7632	0.416	0	27.8656
0.90	−0.0729	−0.6561	−0.1296	31.8843	0.5832	0.0567	31.9572
1.00	0	−0.81	−0.16	36.15	0.81	0.16	36.15

Table 2. Comparing absolute error of an approximate solution with the exact solution for problem 2.

x	Exact value	FPM	HWM	HPM	Error (FPM)	Error (HWM)	Error (HPM)
0.00	0	0	0	0	0	0	0
0.01	0.000101	0.000117	0.00019	0.062957	0.000016	0.000089	0.062856
0.02	0.000408	0.000468	0.00076	0.126228	0.00006	0.000352	0.12582
0.03	0.000927	0.001053	0.00171	0.189813	0.000126	0.000783	0.188886
0.04	0.001664	0.001872	0.00304	0.253712	0.000208	0.001376	0.252048
0.05	0.002625	0.002925	0.00475	0.317925	0.0003	0.002125	0.3153
0.06	0.003816	0.004212	0.00684	0.382452	0.000396	0.003024	0.378636
0.07	0.005243	0.005733	0.00931	0.447293	0.00049	0.004067	0.44205
0.08	0.006912	0.007488	0.01216	0.512448	0.000576	0.005248	0.505536
0.09	0.008829	0.009477	0.01539	0.577917	0.000648	0.006561	0.569088
0.10	0.011	0.0117	0.019	0.6437	0.0007	0.008	0.6327
0.20	0.048	0.0468	0.076	1.3188	0.0012	0.028	1.2708
0.30	0.117	0.1053	0.171	2.0253	0.0117	0.054	1.9083
0.40	0.224	0.1872	0.304	2.7632	0.0368	0.08	2.5392
0.50	0.375	0.2925	0.475	3.5325	0.0825	0.1	3.1575
0.60	0.576	0.4212	0.684	4.3332	0.1548	0.108	3.7572
0.70	0.833	0.5733	0.931	5.1653	0.2597	0.098	4.3323
0.80	1.152	0.7488	1.216	6.0288	0.4032	0.064	4.8768
0.90	1.539	0.9477	1.539	6.9237	0.5913	0	5.3847
1.00	2	1.17	1.9	7.85	0.83	0.1	5.85

Table 3. Comparing absolute error of an approximate solution with the exact solution for problem 3.

x	Exact value	FPM	HWM	HPM	Error (FPM)	Error (HWM)	Error (HPM)
0.00	1	1	1	1	0	0	0
0.01	0.9999	0.999919	0.99992	1.009624	1.8995E−05	1.9995E−05	0.009724
0.02	0.99960008	0.999676	0.99968	1.019296	7.592E−05	7.992E−05	0.01969592
0.03	0.9991004	0.999271	0.99928	1.029016	0.0001706	0.0001796	0.0299156
0.04	0.99840128	0.998704	0.99872	1.038784	0.00030272	0.00031872	0.04038272
0.05	0.99750312	0.997975	0.998	1.0486	0.00047188	0.00049688	0.05109688
0.06	0.99640647	0.997084	0.99712	1.058464	0.00067753	0.00071353	0.06205753
0.07	0.99511199	0.996031	0.99608	1.068376	0.00091901	0.00096801	0.07326401
0.08	0.99362044	0.994816	0.99488	1.078336	0.00119556	0.00125956	0.08471556
0.09	0.99193272	0.993439	0.99352	1.088344	0.00150628	0.00158728	0.09641128
0.10	0.99004983	0.9919	0.992	1.0984	0.00185017	0.00195017	0.10835017
0.20	0.96078944	0.9676	0.968	1.2016	0.00681056	0.00721056	0.24081056
0.30	0.91393119	0.9271	0.928	1.3096	0.01316881	0.01406881	0.39566881
0.40	0.85214379	0.8704	0.872	1.4224	0.01825621	0.01985621	0.57025621
0.50	0.77880078	0.7975	0.8	1.54	0.01869922	0.02119922	0.76119922
0.60	0.69767633	0.7084	0.712	1.6624	0.01072367	0.01432367	0.96472367
0.70	0.61262639	0.6031	0.608	1.7896	0.00952639	0.00462639	1.17697361
0.80	0.52729242	0.4816	0.488	1.9216	0.04569242	0.03929242	1.39430758
0.90	0.44485807	0.3439	0.352	2.0584	0.10095807	0.09285807	1.61354193
1.00	0.36787944	0.19	0.2	2.2	0.17787944	0.16787944	1.83212056

Table 4. Comparing absolute error of an approximate solution with the exact solution for problem 4.

x	Exact value	FPM	HWM	HPM	Error (FPM)	Error (HWM)	Error (HPM)
0.00	0.00	0	0	0	0	0	0
0.01	0.00	1.8E−06	3.2E−06	10.2656	1.8E−06	3.2E−06	10.2656
0.02	0.00	7.2E−06	1.28E−05	20.5824	7.2E−06	1.28E−05	20.5824
0.03	0.00	1.62E−05	2.88E−05	30.9504	1.62E−05	2.88E−05	30.9504
0.04	0.00	2.88E−05	5.12E−05	41.3696	2.88E−05	5.12E−05	41.3696
0.05	0.00	0.000045	0.00008	51.84	4.5E−05	8E−05	51.84
0.06	0.00	6.48E−05	0.000115	62.3616	6.48E−05	0.0001152	62.3616
0.07	0.00	8.82E−05	0.000157	72.9344	8.82E−05	0.0001568	72.9344
0.08	0.00	0.000115	0.000205	83.5584	0.0001152	0.0002048	83.5584
0.09	0.00	0.000146	0.000259	94.2336	0.0001458	0.0002592	94.2336
0.10	0.00	0.00018	0.00032	104.96	0.00018	0.00032	104.96
0.20	0.00	0.00072	0.00128	215.04	0.000719898	0.0012799	215.04
0.30	0.00	0.00162	0.00288	330.24	0.001614095	0.0028741	330.239994
0.40	0.00	0.00288	0.00512	450.56	0.002775142	0.00501514	450.559895
0.50	0.00	0.0045	0.008	576	0.003523438	0.00702344	575.999023
0.60	0.01	0.00648	0.01152	706.56	0.000433382	0.00547338	706.553953
0.70	0.03	0.00882	0.01568	842.24	0.019427525	0.01256752	842.211752
0.80	0.11	0.01152	0.02048	983.04	0.095854182	0.08689418	982.932626
0.90	0.35	0.01458	0.02592	1128.96	0.33409844	0.32275844	1128.61132
1.00	1.00	0.018	0.032	1280	0.982	0.968	1279

Table 5. Comparing absolute error of an approximate solution with the exact solution for problem 5.

x	Exact value	FPM	HWM	HPM	Error (FPM)	Error (HWM)	Error (HPM)
0.00	1	1	1	1	0	0	0
0.01	0.999979	0.999982	0.999984	0.97995	3E−06	5E−06	0.020029
0.02	0.999918	0.999928	0.999936	0.9598	1E−05	1.8E−05	0.040118
0.03	0.999815	0.999838	0.999856	0.93955	2.3E−05	4.1E−05	0.060265
0.04	0.999671	0.999712	0.999744	0.9192	4.1E−05	7.3E−05	0.080471
0.05	0.999486	0.99955	0.9996	0.89875	6.4E−05	0.000114	0.100736
0.06	0.999259	0.999352	0.999424	0.8782	9.3E−05	0.000165	0.121059
0.07	0.998992	0.999118	0.999216	0.85755	0.000126	0.000224	0.141442
0.08	0.998684	0.998848	0.998976	0.8368	0.000164	0.000292	0.161884
0.09	0.998334	0.998542	0.998704	0.81595	0.000208	0.00037	0.182384
0.10	0.998334	0.9982	0.9984	0.795	0.000134	6.6E−05	0.203334
0.20	0.993347	0.9928	0.9936	0.58	0.000547	0.000253	0.413347
0.30	0.985067	0.9838	0.9856	0.355	0.001267	0.000533	0.630067
0.40	0.973546	0.9712	0.9744	0.12	0.002346	0.000854	0.853546
0.50	0.958851	0.955	0.96	−0.125	0.003851	0.001149	1.083851
0.60	0.941071	0.9352	0.9424	−0.38	0.005871	0.001329	1.321071
0.70	0.920311	0.9118	0.9216	−0.645	0.008511	0.001289	1.565311
0.80	0.896695	0.8848	0.8976	−0.92	0.011895	0.000905	1.816695
0.90	0.870363	0.8542	0.8704	−1.205	0.016163	3.7E−05	2.075363
1.00	0.841471	0.82	0.84	−1.5	0.021471	0.001471	2.341471

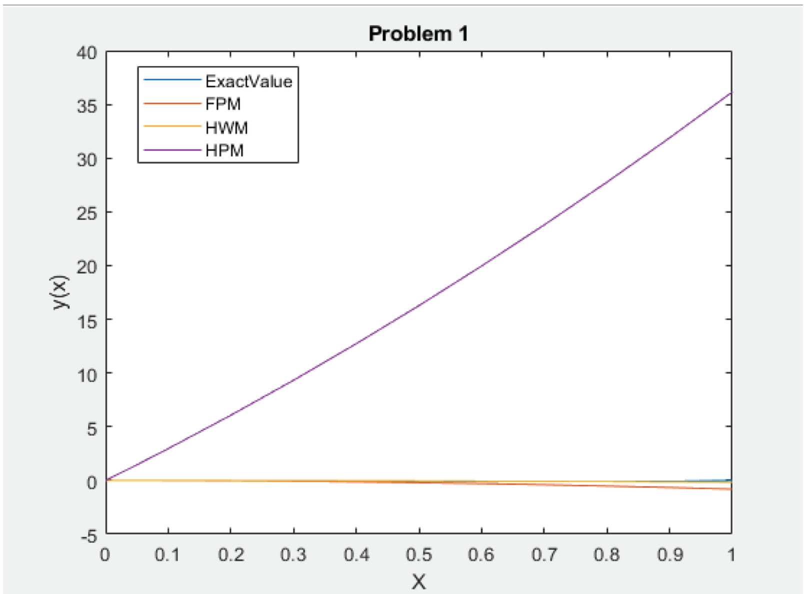

Figure 1. Approximate solution (FPM, HWM, HPM) and exact solution of y(x).

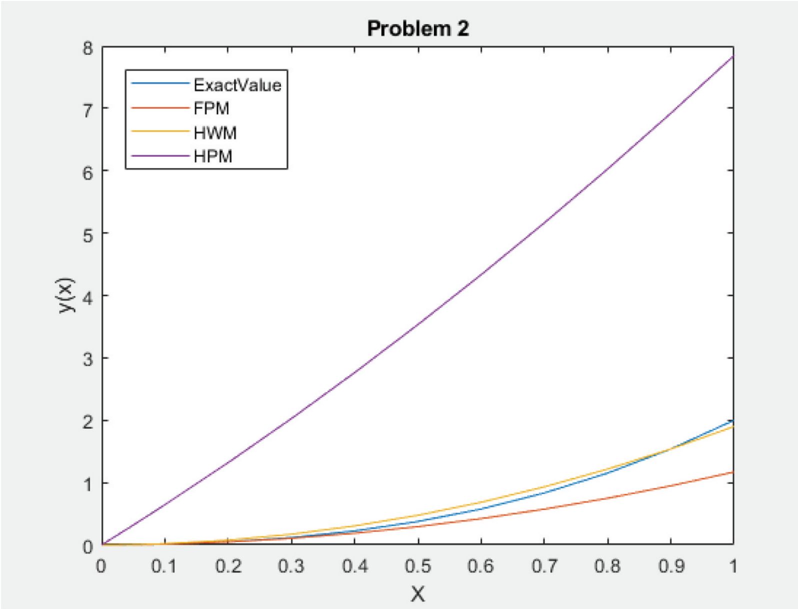

Figure 2. Approximate solution (FPM, HWM, HPM) and exact solution of y(x).

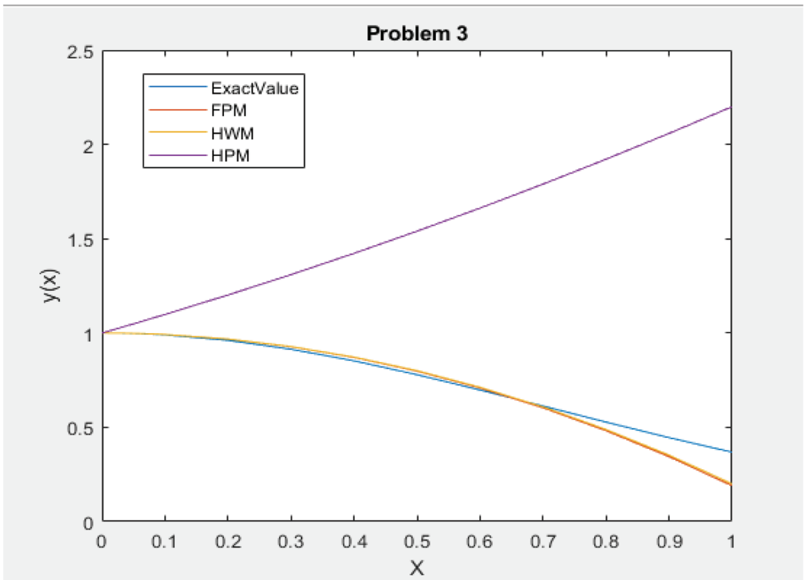

Figure 3. Approximate solution (FPM, HWM, HPM) and exact solution of y(x).

about the metrics analysis like mean, standard deviation, mean square error and accuracy that has been obtained for all the problems. The results demonstrate that the HWM and FPM methods provide highly accurate approximations, with accuracy values reaching close to 1 for most problem instances. In contrast, the accuracy of the HPM methods varies with lower accuracy in certain problems. The Mean Squared Error (MSE) values for the HWM and FPM methods consistently remain very low, where the MSE is near zero, indicating near-perfect approximation. On the other hand, HPM exhibits higher MSE values, especially for more complex problems like Problem 4, where the error magnitude increases significantly, reflecting the limitations of polynomial approximation techniques. Operational matrix of derivative algorithms has been frequently used for solving non-linear differential equations. Hermite, Hosoya and Fermat polynomial algorithms have been identified to solve non-linear differential equations in engineering. Among a few wavelet families, the proposed algorithms have been identified as useful tools in solving non-linear models in scientific and engineering

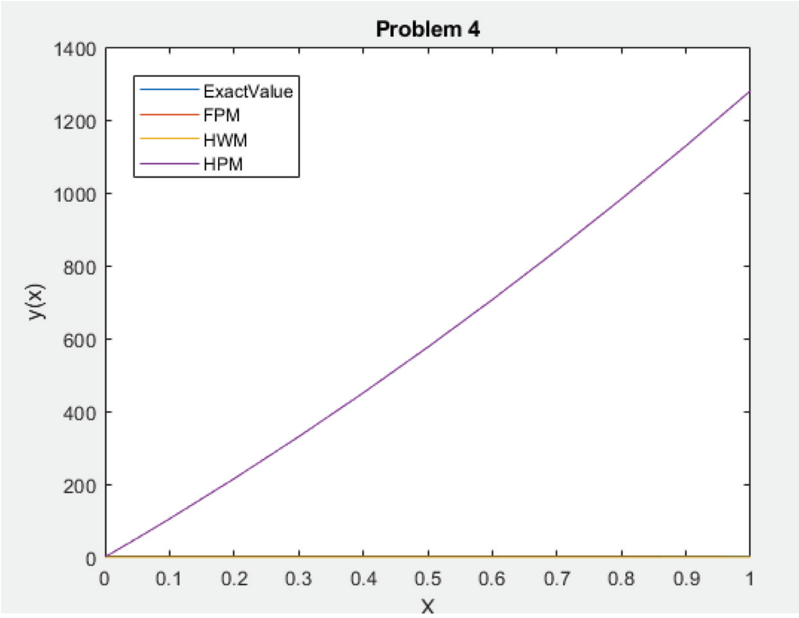

Figure 4. Approximate solution (FPM, HWM, HPM) and exact solution of y(x).

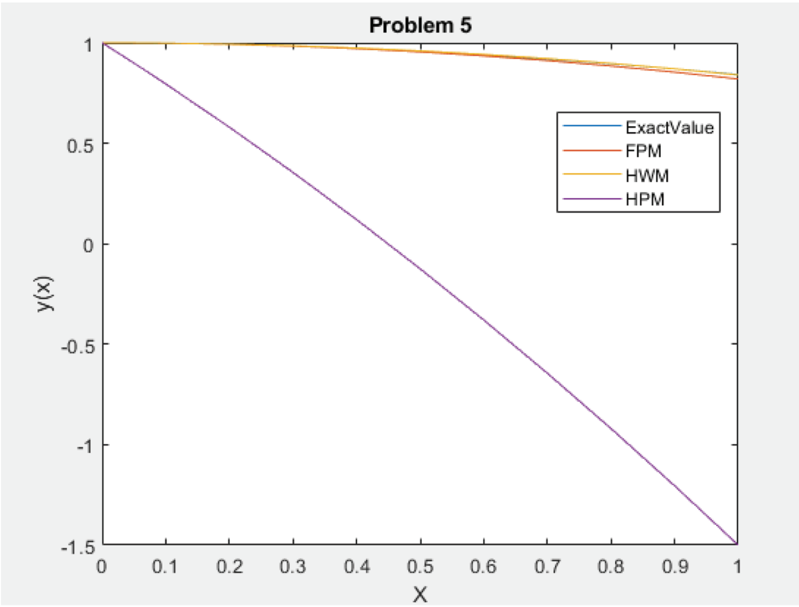

Figure 5. Approximate solution (FPM, HWM, HPM) and exact solution of y(x).

applications. For specific models (as mentioned in the manuscript), these algorithms have been identified as useful tools for solving non-linear dynamical models.

5. Conclusion

Two reliable and efficient wavelet-based methods have been introduced successfully for solving non-linear Lane–Emden-type equations in astrophysics. The operational matrix of derivatives has been utilised to convert the non-linear differential equations into a system of algebraic equations. Validation with other polynomial approximation methods has been noticed. Due to the sparse type of matrices, the computational time is much less when compared with other conventional methods. The proposed methods also show better stability and consistency in their error behaviour across various problems, making them a more reliable tool for solving non-linear differential equation models. Overall, these

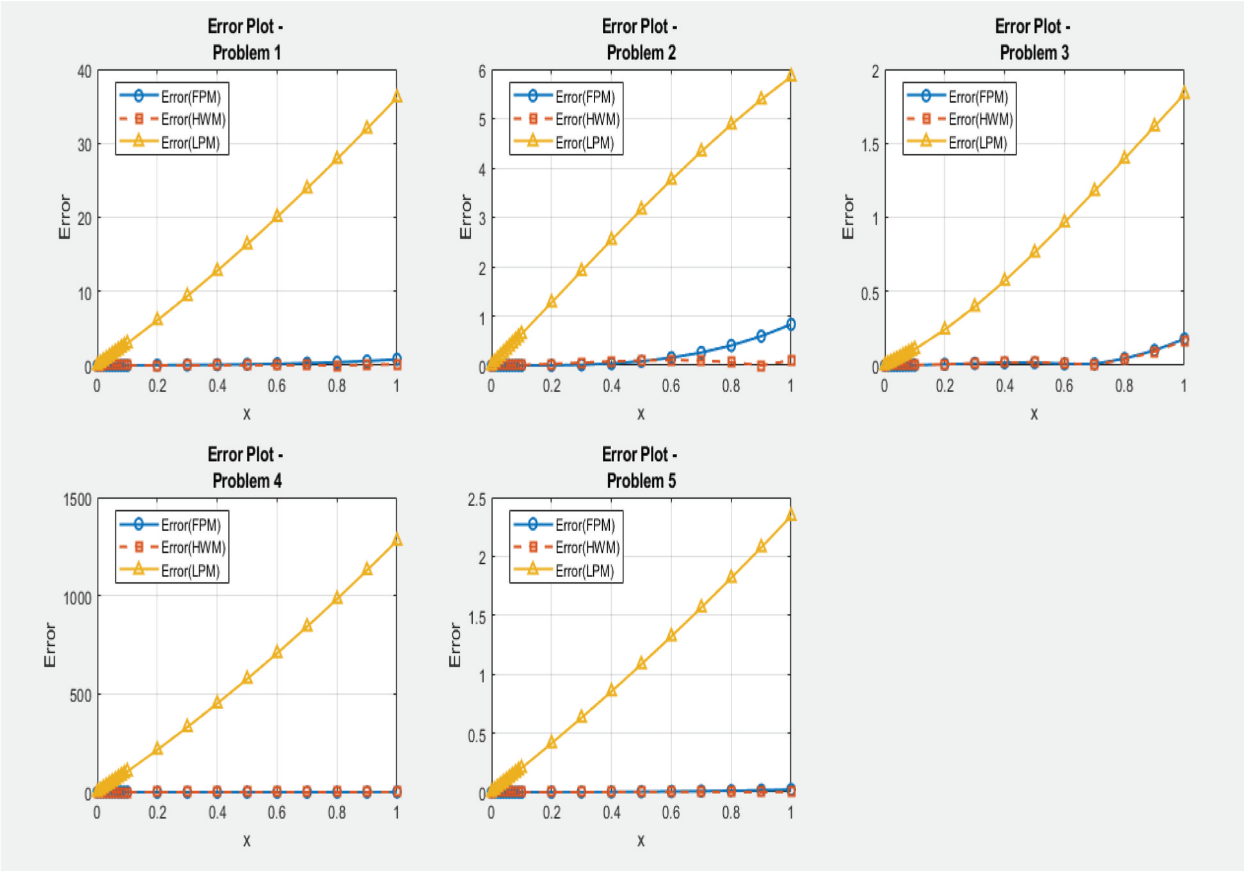

Figure 6. Graphical representation of error analysis for all the cases.

Table 6. Metric analysis for FPM.

Problem	Mean_FPM	STD_FPM	MSE_FPM	Accuracy_FPM
Problem1	0.1324	0.22698	0.066473	0.88308
Problem2	0.11874	0.23157	0.065041	0.89387
Problem3	0.020445	0.043937	0.0022519	0.97996
Problem4	0.072057	0.22731	0.054277	0.93279
Problem5	0.0036394	0.0061904	0.00004965	0.99637

Table 7. Metric analysis for HWM.

Problem	Mean_HWM	STD_HWM	MSE_HWM	Accuracy_HWM
Problem1	0.015659	0.037015	0.0015468	0.98458
Problem2	0.033181	0.04206	0.0027816	0.96788
Problem3	0.019444	0.041115	0.001984	0.98093
Problem4	0.070656	0.22351	0.052451	0.93401
Problem5	0.0004594	0.0005085	4.5669E−07	0.99954

Table 8. Metric analysis for HPM.

Problem	Mean_HPM	STD_HPM	MSE_HPM	Accuracy_HPM
Problem1	10.03	11.815	233.22	0.090658
Problem2	1.8275	2.004	7.1548	0.35367
Problem3	0.47626	0.60026	0.56912	0.67739
Problem4	354.21	417.2	290820	0.0028152
Problem5	0.66062	0.76729	0.99571	0.60218

methods provide a more accurate, stable and scalable approach compared to traditional polynomial methods, highlighting their potential in tackling complex problems in science and engineering. The proposed methods are reliable approximation algorithms for solving non-linear differential equation models arising in various scientific and engineering problems.

Acknowledgements

The authors are thankful to SASTRA Deemed University in Thanjavur for providing infrastructure support to carry out this research. We also acknowledge the SPARC-MHRD (Project Code: P3755) and DST-SERB (CRG Grant) File Number: CRG/2023/002736, New Delhi for financial support.

Disclosure statement

No potential conflict of interest was reported by the author(s).

Funding

This work was supported by the Science and Engineering Research Board [CRG/2023/002736].

References

Abu Arqub O, Ahmad El-Ajou ASB, Hashim I, Hashim I. 2013. A representation of the exact solution of generalized Lane-Emden equations using a new analytical method, Hindawi publishing corporation. Abstract Appl Anal. 2013:1–10. doi: 10.1155/2013/378593.

Ali MR. 2019. A new algorithm for solving the nonlinear lane–Emden equations arising in astrophysics, 1 (183):2523-3971. doi:10.1007/s42452-019-0173-5.

Baty H. 2023. July. Modelling Lane–Emden type equations using Physics-Informed Neural Networks. Astron Comput. 44:100734. doi: 10.1016/j.ascom.2023.100734.

Biswas A, Mondal S, Chatterjee A. 2023. May. Subhabrata Mondal and Ayan Chatterjee, solution of Lane-Emden type differential equations by using differential transform method. J Mines Met Fuels. 698–702. doi: 10.18311/jmmf/2023/34173.

Gireesha BJ, Gowtham KJ. 2024. Efficient hypergeometric wavelet approach for solving Lane-Emden equations. J Comput Sci. 82:102392. doi: 10.1016/j.jocs.2024.102392.

Mukherjee S, Roy B. 2011. Solution of Lane-Emden equation by differential transform method. Int J Nonlinear Sci. 12(4):478–484.

Nduka MU, Oruh BI. 2022. May. A Fermat polynomial method for solving optimal control problems. Int J Math Anal Modell. 5(1):56–68.

Parand K, Mehdi Dehghan ARR, Ghaderi SM, Ghaderi SM. 2010. June. An approximation algorithm for the solution of the nonlinear Lane–Emden type equations arising in astrophysics using Hermite functions collocation method. Comput Phys Commun. 181(6):1096–1108. doi: 10.1016/j.cpc.2010.02.018.

Youssri YH. 2017. A new operational matrix of Caputo fractional derivatives of Fermat polynomials: an application for solving the Bagley-Torvik equation. Youssri Adv Diff Eqs. 2017(1):73. doi: 10.1186/s13662-017-1123-4.

ZdeněkŠmarda Y. 2015. Dec 15. Anefficientcomputational approachtosolvingsingular initialvalueproblemsforLane–emdentypeequations. J Com Appl Math. 290:65–73.